Astron. Astrophys. 359, 788–798 (2000)

ASTRONOMY AND ASTROPHYSICS

The diffusion of radiation in moving media

II. Limits for large and small velocity gradients for deterministic lines

R. Wehrse[1,3]**, B. Baschek**[1,3]**, and W. von Waldenfels**[2,3]

[1] Institut für Theoretische Astrophysik, Tiergartenstrasse 15, 69121 Heidelberg, Germany
[2] Institut für Angewandte Mathematik, Im Neuenheimer Feld 294, 69120 Heidelberg, Germany
[3] Interdisziplinäres Zentrum für Wissenschaftliches Rechnen, Im Neuenheimer Feld 368, 69120 Heidelberg, Germany

Received 18 January 2000 / Accepted 27 April 2000

Abstract. The general formulae for radiative quantities in the diffusion limit for a differentially moving 3D medium which have been derived in Paper I of this series, are evaluated for the limiting cases of very large and very small velocity gradients $|w|$. The extinction coefficient is specified by the continuum and the contribution of spectral lines which is formulated deterministically. For large w all radiative quantities can conveniently be calculated in terms of the spectral thickness, i.e. of the wavelength-integrated extinction coefficient, which can be well approximated by a piecewise linear function. For small w the radiative quantities are developed to the second order in w. The coefficients are essentially determined by the first two wavelength derivatives of the mean free path of the photons, i.e. of the reciprocal extinction coefficient. Since these depend on temperature, density and chemical composition only, they can be precalculated resulting in convenient expressions for hydrodynamic calculations. Examples are given for selected extinction coefficients such as a power-law continuum, a spectral edge, a single narrow line, and many, isolated as well as overlapping lines. In the non-overlapping case the lines contribute only in second order of w and the motions always lead to a decrease of the total flux whereas the radiative acceleration is unaffected. On the other hand, the effect of overlapping lines can only be determined by a detailed calculation for any specific extinction distribution. Furthermore, it is shown that the flux vector has components perpendicular to the temperature gradient if the latter is not parallel to the velocity vector.

Key words: diffusion – radiative transfer – stars: interiors – stars: novae, cataclysmic variables – stars: supernovae: general

1. Introduction

The comoving-frame radiative transfer equation has been derived and solved by Wehrse et al. (2000) (Paper I of this series) for differential motions (with velocities much smaller than the speed of light) in a medium which is optically thick so that the diffusion limit of the radiation applies, and expressions for radiative quantities such as the wavelength-integrated flux and radiative acceleration have been given. These expressions become particularly simple if the absolute value of the velocity gradient $|w|$ is either very large or very small, and if the extinction due to the spectral lines can be described in a determinisitic way. In the present Paper (II) a detailed derivation and discussion of the radiative quantities for these two limiting cases is given; preliminary results have already been reported in a review-like paper by Wehrse & Baschek (1999).

We first formulate, in this Introduction, the conditions for the validity of the limiting cases of large and small w, respectively. In Sect. 2, we then recall some basic results from Paper I and describe the deterministic extinction coefficient used here. For a complete list of the assumptions made and for the notation, we refer to Paper I; an equation (n) of that paper is cited here by (I:n). Subsequently we treat the limiting case of large w in Sect. 3, and - in much more detail – that for small w in Sect. 4. For the latter, more important case the effects of the motions are demonstrated by selected examples of extinction coefficients: a power-law continuum, a spectral edge, a narrow single line, and many, isolated as well as overlapping lines. While in the previous sections the flux is considered only in a given direction, Sect. 5 is devoted to the intricate behavior of the flux *vector* if the directions of the temperature gradient and of the velocity gradient do not coincide. The essential featurers of these anisotropic mean free photon paths are demonstrated for a plane-parallel stratification in the limit of small w. Finally, the conclusions and an outlook are given in Sect. 6.

The *limiting cases* of a large or a small velocity gradient are realized if the Doppler shift $\delta\xi_{\rm D}$ occurring over a mean free path length in the continuum is much larger or much smaller than the intrinsic width $\Delta\xi_{\rm line}$ of the narrowest spectral line, i.e. if

$$|\delta\xi_{\rm D}| \gg \Delta\xi_{\rm line} \qquad \text{or} \qquad |\delta\xi_{\rm D}| \ll \Delta\xi_{\rm line}\,, \tag{1}$$

respectively. Here we have expressed shifts and line widths in the logarithmic wavelength scale $\xi = \ln\lambda$ (I:3) which we use throughout this paper.

We express the Doppler shift $\delta\xi_{\rm D}$ in terms of the velocity gradient (I:33)

$$w \simeq \mathbf{n}\cdot\nabla(\boldsymbol{\beta}\cdot\mathbf{n}) = \frac{d(\mathbf{n}\cdot\boldsymbol{\beta})}{ds} \tag{2}$$

Send offprint requests to: R. Wehrse (wehrse@ita.uni-heidelberg.de)

with s being the path element in the ray direction. Since the mean free path of a photon in the continuum is $1/\chi_{\rm c}$ with $\chi_{\rm c}$ being the continuous extinction coefficient, the change of the velocity $\delta\beta = \delta v/c$ (c velocity of light) over a mean free path is $w/\chi_{\rm c}$, and hence $\delta\xi_{\rm D} = \delta\lambda_{\rm D}/\lambda = \delta\beta \simeq w/\chi_{\rm c}$. On the other hand, the intrinsic line width $\Delta\xi_{\rm line}$ is of the order either of the damping constant γ (in the ξ scale) for a Lorentz profile (Eq. (10)) or of the Doppler width W for a Gauss and for a Voigt profile (Eq. (11)).

In this paper we adopt mostly *Lorentz* profiles for the discussion of our examples so that the limiting cases (1) imply for the velocity gradient

$$|w| \gg \gamma \cdot \chi_{\rm c} \qquad \text{or} \qquad |w| \ll \gamma \cdot \chi_{\rm c}\,, \tag{3}$$

respectively. In the *diffusion* limit the condition $|w| \ll \chi_{\rm c}$ (I:34), of course, is fulfilled in addition.

2. Basic expressions

2.1. Monochromatic radiation flux

The monochromatic flux vector $\mathbf{F}(s_0,\xi)$ at depth s_0 is obtained by integration over all directions (I:12) from the flux $\mathcal{F}(s_0,\xi)$ in the direction **n**(I:13). In the diffusion limit we write the latter for a moving medium in the form (I:42)

$$\mathcal{F}(s_0,\xi;w) = \mathcal{F}(s_0,\xi)\cdot\Big[1+\theta(s_0,\xi;w)\Big] \tag{4}$$

with $\mathcal{F}(s_0,\xi) = 2g(s_0,\xi,\mathbf{n})/\chi(\xi)$ being the corresponding static value, so that the correction (I:44) for the inclusion of a velocity field is

$$1+\theta(s_0,\xi;w) = \chi(\xi)\int_0^\infty \exp\left(-\frac{\psi(\xi)-\psi(\xi-ws)}{w}\right)ds. \tag{5}$$

Here $\chi(\xi)$ is the monochromatic extinction coefficient, $\psi(\xi)$ the corresponding spectral thickness (I:37) with $\psi' \equiv d\psi/d\xi = \chi(\xi)$,

$$g(s_0,\xi,\mathbf{n}) = \frac{\partial B(T,\xi)}{\partial T}\,\mathbf{n}\cdot\nabla T = \left.\frac{\partial B(T,\xi)}{\partial T}\frac{\partial T}{\partial s}\right|_{s_0} \tag{6}$$

the spatial derivative (I:6) of the the Planck function $B(T,\xi)$ for the temperature $T = T(s_0)$ at depth s_0, and

$$G(s_0,\xi) = \left.\left(\frac{\partial B(T,\xi)}{\partial T}\Big/\frac{\partial B(T)}{\partial T}\right)\right|_{s_0}\cdot\,{\rm e}^{\xi} \tag{7}$$

the weighting function (I:8) entering the Rosseland mean opacity. $B(T)$ is the wavelength integrated Planck function, and $\partial B(T)/\partial T = 4\sigma_{\rm SB}T^3/\pi$ ($\sigma_{\rm SB}$ Stefan-Boltzmann constant).

As has been shown in Sect. 5 of Paper I, other radiative quantities of interest, in particular the monochromatic radiative acceleration $a_{\rm rad}$ (I:16), as well as the wavelength-integrated expressions (I:11,15) can be derived from the monochromatic flux.

2.2. Extinction coefficient

The extinction coefficient copmprising absorption and scattering – can be written in the *deterministic* description – as the sum of a continuous part $\chi_{\rm c}$ and the contribution of the individual spectral lines, denoted by the subscript l,

$$\chi(\xi) = \chi_{\rm c}(\xi) + \sum_l \chi_l(\xi) = \chi_{\rm c}(\xi) + \sum_l A_l\Phi_l(\xi-\xi_l) \tag{8}$$

with A_l being the strength of the line l at the position ξ_l, and $\Phi_l(\xi-\xi_l)$ its profile function, normalized to $\int_{\rm line}\Phi_l(\xi-\xi_l)d\xi = 1$, and the assumption that $\chi_{\rm c}$ does not vary significantly over the range of any given spectral line. The corresponding spectral thickness is

$$\psi(\xi) = \psi_{\rm c}(\xi) + \sum_l \psi_l(\xi)\,. \tag{9}$$

For the profile function Φ we may choose either Lorentz L or Doppler D profiles, which – in the dimensionless logarithmic wavelength scale – read

$$\Phi_l(\xi-\xi_l) \equiv L_l(\xi-\xi_l) = \frac{1}{\pi}\,\frac{\gamma_l/2}{(\xi-\xi_l)^2+(\gamma_l/2)^2} \tag{10}$$

and

$$\Phi_l(\xi-\xi_l) \equiv D_l(\xi-\xi_l) = \frac{1}{\sqrt{\pi}\,W_l}\,\exp\left[-\left(\frac{\xi-\xi_l}{W_l}\right)^2\right], \tag{11}$$

respectively. If the line is sufficiently narrow, i.e. if the relevant distances $|\xi-\xi_l|$ from the line center are not too large, the profile functions are obtained from the conventional profiles $\hat\Phi$ by utilizing $\Phi(\xi-\xi_l)d\xi = \hat\Phi(\lambda-\lambda_l)d\lambda$ (cf. Appendix B of Wehrse et al. 1998); furthermore $\gamma_l = \hat\gamma_l/\lambda_l$ and $W_l = \hat W_l/\lambda_i$ where $\hat\gamma_l$ and $\hat W_l$ are the usual damping constant and Doppler width, respectively, in the ordinary wavelength scale.

In astrophysical applications one frequently has to treat a *very large* number of spectral lines. In this case one can, on the one hand, choose to apply large lists of "real" lines which may result in very time-consuming calculations, if this is possible at all. On the other hand, the deterministic treatment of very many lines may be replaced by a *statistic* approach. As Wehrse et al. (1998) have shown, the distribution of spectral lines can well be described by a Poisson point process. The effects in the diffusion limit will be discussed in a subsequent paper of this series.

3. Limit of large w

We now consider the limiting case of *large* w when the Doppler shift occurring over a mean free path length of a photon in the continuum is much larger than the intrinsic line width, i.e. $|w| \gg \gamma\chi_{\rm c}$ (Eq. (3)).

According to Baschek et al. (1997), the spectral thickness is essentially a piecewise linear function, and the importance of deviations from the piecewise linear functions decreases with increasing $|w|$. This presentation is particularly useful if very

many spectral lines have to be taken into account for the extinction coefficient, but is also valid for isolated narrow lines.

The *simplest* case is $\psi(\xi) = a\xi$ over the entire spectrum, which corresponds to an extinction coefficient $\chi = \psi' = a$ which is independent of ξ. The resulting flux is

$$\mathcal{F}(s_0, \xi; w) = \frac{2g(s_0, \xi, \mathbf{n})}{a}\,, \tag{12}$$

i.e. it does not depend on the velocity.

Whenever there is a break in $\psi(\xi)$, the integral in (5) has to be split. For example, if we consider a change in slope at ξ_0 from a_1 to a_2 as well as a jump $\Delta\psi$, i.e.

$$\psi(\xi) = \begin{cases} a_1\xi & \text{for} \quad \xi < \xi_0 \\ a_1\xi_0 + a_2(\xi - \xi_0) + \Delta\psi & \text{for} \quad \xi \geq \xi_0 \end{cases}\,, \tag{13}$$

the resulting flux for any $\xi > \xi_0$ is

$$\begin{aligned} &\mathcal{F}(s_0, \xi; w) = \\ &2g(s_0, \xi, \mathbf{n})\left(\frac{1 - \mathrm{e}^{-a_2(\xi-\xi_0)/w}}{a_2} + \frac{\mathrm{e}^{-a_2(\xi-\xi_0)/w}\,\mathrm{e}^{-\Delta\psi/w}}{a_1}\right) \\ &= \frac{2g(s_0, \xi, \mathbf{n})}{a_2}\left[1 - \mathrm{e}^{-a_2(\xi-\xi_0)/w}\left(1 - \frac{a_2}{a_1}\,\mathrm{e}^{-\Delta\psi/w}\right)\right]. \end{aligned} \tag{14}$$

Evidently, the use of the piecewise linear approximation speeds up actual calculations by a very large factor (cf. Baschek et al. 1997).

4. Limit of small w

With the assumption that ψ is sufficiently smooth we may – keeping the line width γ fixed – expand the exponential in Eq. (5) in terms of w to second order,

$$\begin{aligned} &\exp\left(-\frac{\psi(\xi) - \psi(\xi - ws)}{w}\right) \\ &\simeq \mathrm{e}^{-\psi'(\xi)\cdot s}\left[1 + \frac{1}{2}s^2\psi''(\xi)\,w \right. \\ &\qquad \left. + \left(\frac{1}{8}s^4\psi''(\xi)^2 - \frac{1}{6}s^3\psi'''(\xi)\right)w^2\right] + O(w^3) \end{aligned} \tag{15}$$

and obtain for the "w correction factor" to second order in w

$$\begin{aligned} &1 + \theta(s_0, \xi; w) = \\ &\frac{\chi(\xi)}{\psi'(\xi)}\left[1 + \frac{\psi''(\xi)}{\psi'(\xi)^2}\,w + \frac{1}{\psi'(\xi)^3}\left(3\frac{\psi''(\xi)^2}{\psi'(\xi)} - \psi'''(\xi)\right)w^2\right]. \end{aligned} \tag{16}$$

Replacing $\psi'(\xi)$ by $\chi(\xi)$ etc. again, the flux in the diffusion limit becomes

$$\begin{aligned} &\mathcal{F}(s_0, \xi; w) \\ &= \mathcal{F}(s_0, \xi)\cdot\left[1 - \frac{\partial}{\partial\xi}\frac{1}{\chi(\xi)}\cdot w + \frac{1}{2}\frac{\partial^2}{\partial\xi^2}\frac{1}{\chi(\xi)^2}\cdot w^2\right]. \end{aligned} \tag{17}$$

From this expression we realize that, while the static part of the monochromatic flux is determined only by the (monochromatic) extinction coefficient $1/\chi(\xi)$ or, equivalently, by the mean free path $1/\chi(\xi)$, the effect of the differential *motions* is – to second order in w – determined by the first two wavelength *derivatives* of the mean free path of the photons and, of course, by the gradient w itself.

4.1. Wavelength-integrated radiative quantities

With Eq. (17) we obtain for the wavelength integrated (total) *flux* (I:45)

$$\mathcal{F}_{\rm tot}(s_0; w) = \mathcal{F}_{\rm tot}(s_0)\cdot\left[1 + \eta_1(s_0)\cdot w + \eta_2(s_0)\cdot w^2\right], \tag{18}$$

and correspondingly for the *generalized Rosseland mean opacity* (I:50)

$$\frac{1}{\bar\chi_\beta(s_0; w)} = \frac{1}{\bar\chi_{\rm R}(s_0)}\cdot\left[1 + \eta_1(s_0)\cdot w + \eta_2(s_0)\cdot w^2\right], \tag{19}$$

with the coefficients

$$\begin{aligned} \eta_1(s_0) &= -\bar\chi_{\rm R}(s_0)\int_{-\infty}^{\infty}\frac{1}{\chi(\xi)}\frac{\partial}{\partial\xi}\left(\frac{1}{\chi(\xi)}\right)G(s_0,\xi)\,d\xi \\ &= -\frac{1}{2}\,\bar\chi_{\rm R}(s_0)\int_{-\infty}^{\infty}\frac{\partial}{\partial\xi}\left(\frac{1}{\chi(\xi)}\right)^2 G(s_0,\xi)\,d\xi\,, \end{aligned} \tag{20}$$

$$\eta_2(s_0) = +\frac{1}{2}\,\bar\chi_{\rm R}(s_0)\int_{-\infty}^{\infty}\frac{1}{\chi(\xi)}\frac{\partial^2}{\partial\xi^2}\left(\frac{1}{\chi(\xi)}\right)^2 G(s_0,\xi)\,d\xi\,. \tag{21}$$

Here $\mathcal{F}_{\rm tot}(s_0)$ and $\bar\chi_{\rm R}(s_0)$ are the corresponding static quantities, and $G(s_0, \xi)$ is the weighting function defined by Eq. (7).

The total *radiative acceleration* (I:46) becomes

$$\begin{aligned} &a_{\rm rad,tot}(s_0; w) \\ &\quad = a_{\rm rad,tot}(s_0)\cdot\left[1 + \tilde\eta_1(s_0)\cdot w + \tilde\eta_2(s_0)\cdot w^2\right] \end{aligned} \tag{22}$$

with $a_{\rm rad,tot}(s_0)$ being the static value and

$$\tilde\eta_1(s_0) = -\int_{-\infty}^{\infty}\frac{\partial}{\partial\xi}\left(\frac{1}{\chi(\xi)}\right)G(s_0,\xi)\,d\xi\,, \tag{23}$$

$$\tilde\eta_2(s_0) = \frac{1}{2}\int_{-\infty}^{\infty}\frac{\partial^2}{\partial\xi^2}\left(\frac{1}{\chi(\xi)}\right)^2 G(s_0,\xi)\,d\xi\,. \tag{24}$$

Since the η_k and $\tilde\eta_k$ are functions of temperature, density, and chemical composition only, they may be precalculated once for all so that we have – for *small* velocity gradients w – derived a convenient form of the radiative quantities for actual radiation-hydrodynamical calculations.

4.2. Effects of various extinction distributions

In order to understand the various terms given above in some detail we now discuss several special cases of the extinction coefficient which may be regarded as basic building blocks for more general extinction distributions.

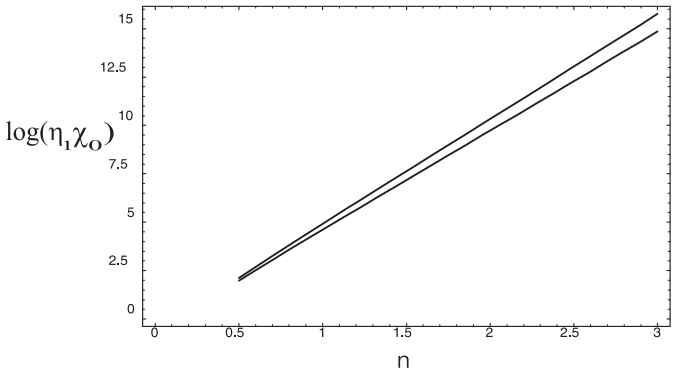

Fig. 1. First-order coefficient $\log(\eta_1 \cdot \chi_0)$ of the total flux for the power-law continuum $\chi(\xi) = \chi_0 \exp(n\xi)$ as a function of the index n. Curves for temperatures of 10^4 and $2 \cdot 10^4$ K.

4.2.1. Power-law continuum

Let us start with a continuum obeying a power law in wavelength, i.e.

$$\chi(\xi) = \chi_0 \, \mathrm{e}^{n\xi} \, . \tag{25}$$

In this case the static Rosseland opacity is $\bar{\chi}_{\mathrm{R}}(s_0) = \chi_0 / \int_{-\infty}^{\infty} \exp(-n\xi) G(s_0, \xi) d\xi$. With these expressions we find for the coefficients of the flux (18) and the radiative acceleration (22)

$$\eta_k(s_0) = \frac{k\, n^k}{\bar{\chi}_{\mathrm{R}}(s_0)^k} \frac{\int_{-\infty}^{\infty} \exp(-(k+1)n\xi)\, G(s_0, \xi) d\xi}{\left[\int_{-\infty}^{\infty} \exp(-n\xi)\, G(s_0, \xi) d\xi\right]^{k+1}} \qquad (k = 1, 2) \tag{26}$$

and

$$\tilde{\eta}_k(s_0) = \frac{k\, n^k}{\bar{\chi}_{\mathrm{R}}(s_0)^k} \frac{\int_{-\infty}^{\infty} \exp(-kn\xi)\, G(s_0, \xi) d\xi}{\left[\int_{-\infty}^{\infty} \exp(-n\xi)\, G(s_0, \xi) d\xi\right]^{k}} \qquad (k = 1, 2). \tag{27}$$

Surprisingly, the coefficient of the linear term ($k = 1$) for the radiative acceleration reduces to

$$\tilde{\eta}_1(s_0) = \frac{n}{\bar{\chi}_{\mathrm{R}}(s_0)} \, . \tag{28}$$

Thus in a differentially moving configuration with a power law extinction the flux increases super-exponentially with n (Fig. 1) and the acceleration only linearly.

Note that a direct evaluation of $\mathcal{F}(s_0, \xi; w)$ from (4) and (I:39) leads to divergences for the power-law wavelength distribution of the extinction coefficient (25) since at some wavelength the configuration starts to become optically thin and our basic assumptions are no longer valid. However, already the addition of an arbitrarily small wavelength independent extinction removes this problem.

4.2.2. Spectral edge

Here we consider an edge superimposed on a wavelength independent continuum and restrict ourselves here to the *first order* terms since they already give non-negligible contributions. We approximate the edge by the tangent hyperbolic function

$$\chi(\xi) = \chi_{\mathrm{c}} + \chi_{\mathrm{e}} \left(1 + \tanh \frac{\xi_0 - \xi}{\delta}\right) , \tag{29}$$

i.e. we consider a "jump" of *finite* width $\delta > 0$ and total height $2\chi_{\mathrm{e}}$ (Fig. 2a). We note that although the edge $\chi(\xi)$ is symmetric with respect to $\xi = 0$, its derivatives are not.

In order to determine the *contribution* of the edge to the wavelength integrated quantities we integrate from $\xi_0 - m\delta$ to $\xi_0 + m\delta$ ($m > 0$). Note that the weighting function G varies only very little over the edge and therefore can be approximated by a constant. The relevant integrals are found to be

$$\int_{\xi_0 - m\delta}^{\xi_0 + m\delta} \frac{\partial}{\partial \xi} \frac{1}{\chi(\xi)^2} d\xi = \left. \frac{1}{\chi(\xi)^2} \right|_{\xi_0 - m\delta}^{\xi_0 + m\delta} = \frac{1}{[\chi_{\mathrm{c}} + \chi_{\mathrm{e}}(1 - \tanh(m))]^2} - \frac{1}{[\chi_{\mathrm{c}} + \chi_{\mathrm{e}}(1 + \tanh(m))]^2} > 0 \tag{30}$$

for the monochromatic flux and

$$\int_{\xi_0 - m\delta}^{\xi_0 + m\delta} \frac{\partial}{\partial \xi} \frac{1}{\chi(\xi)} d\xi = \left. \frac{1}{\chi(\xi)} \right|_{\xi_0 - m\delta}^{\xi_0 + m\delta} = \frac{1}{\chi_{\mathrm{c}} + \chi_{\mathrm{e}}(1 - \tanh(m))} - \frac{1}{\chi_{\mathrm{c}} + \chi_{\mathrm{e}}(1 + \tanh(m))} > 0 \tag{31}$$

for the monochromatic radiative acceleration; the corresponding coefficients η_1 and $\tilde{\eta}_1$ are negative.

These expressions show that both the flux as well as the radiative acceleration may be reduced or increased depending on the sign of w and that the amount of the change is independent of the sharpness δ of the edge.

4.2.3. Single narrow line

Next we treat the effects of a narrow single line of Lorentzian shape, a case which we have discussed already in a different context in Paper I, writing the extinction coefficient (I:51) in the form

$$\chi(\xi) = \chi_{\mathrm{c}} + A \cdot \Phi(\xi) = \chi_{\mathrm{c}} + A \, \frac{\gamma/(2\pi)}{(\xi - \xi_0)^2 + (\gamma/2)^2} \, . \tag{32}$$

In order to evaluate the effect of the motions (in the limit of small w) on the wavelength-integrated radiative flux and acceleration, the derivatives

$$\frac{\partial}{\partial \xi} \frac{1}{\chi(\xi)} = \frac{4\pi}{\gamma} (\xi - \xi_0) \frac{A\Phi^2}{\chi^2} \, , \tag{33}$$

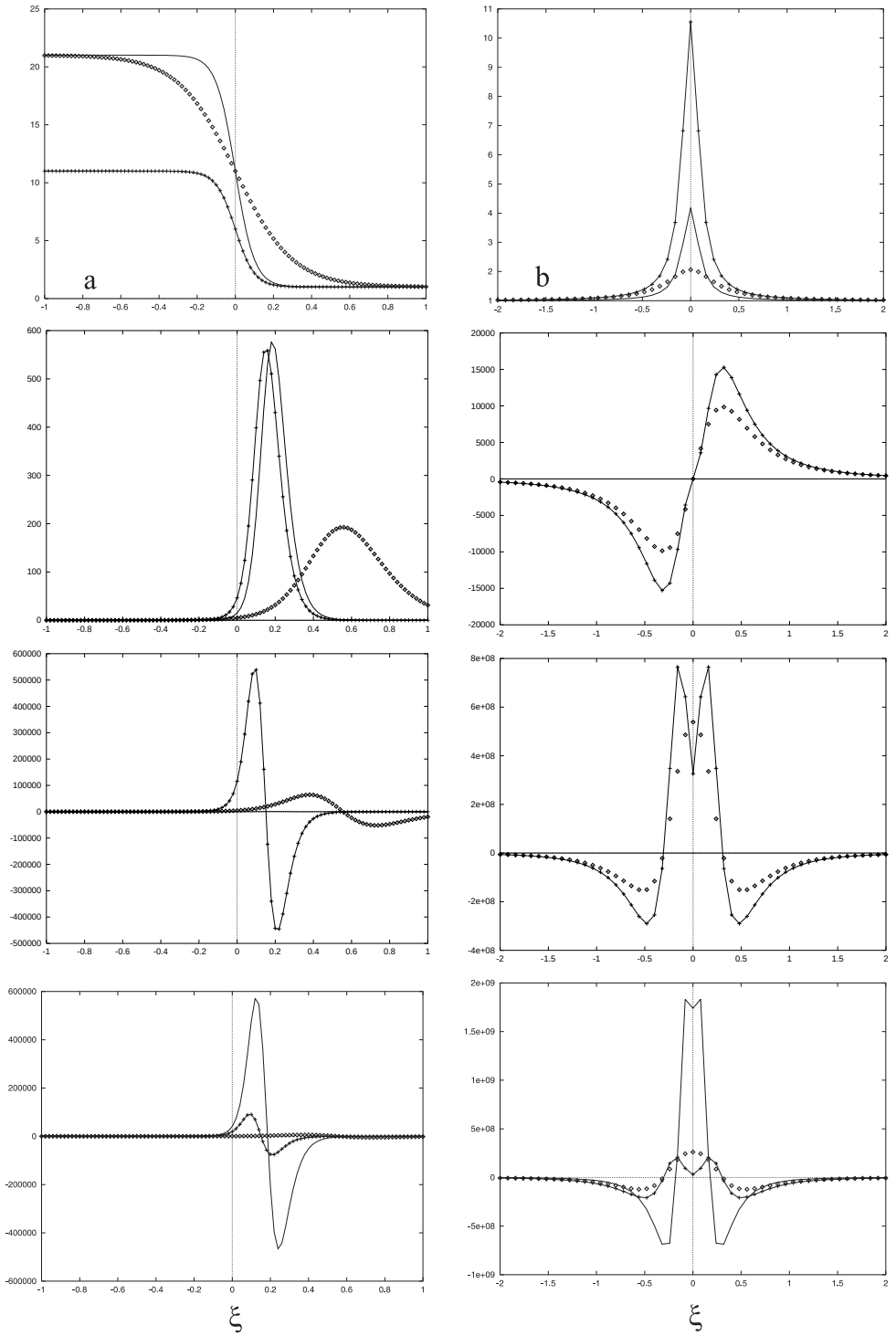

Fig. 2a and b. Examples for the behavior of the extinction coefficients χ (*top row*) and the derivatives of the corresponding free mean paths $\partial(1/\chi(\xi)^2)/\partial\xi$, $\partial^2(1/\chi(\xi)^2)/\partial\xi^2$, $\partial^2(1/\chi(\xi)^2)/\partial\xi^2/\chi(\xi)$ (*2nd row to bottom*) contributing to the velocity-dependent terms of Eqs. 20, 24, 21 as functions of ξ: **a** Spectral edge of $\tanh$ shape, see Eq. (29), with $\chi_e = 10$, $\delta = 0.001$ (full curve), $\chi_e = 10$, $\delta = 0.003$ (crossed curve), $\chi_e = 5$, $\delta = 0.001$ (diamonds) on a continuum $\chi_c = 1$; **b** single Lorentzian line with $A = 10^{-4}$, $\gamma = 10^{-5}$ (full curve), $A = 10^{-4}$, $\gamma = 3 \cdot 10^{-5}$ (crossed curve), $A = 3 \cdot 10^{-4}$, $\gamma = 10^{-5}$ (diamonds) also on a continuum $\chi_c = 1$, see Eq. (32).

$$\frac{\partial}{\partial\xi}\frac{1}{\chi(\xi)^2} = \frac{8\pi}{\gamma}(\xi-\xi_0)\frac{A\Phi^2}{\chi^3}\,, \tag{34}$$

$$\frac{\partial^2}{\partial\xi^2}\frac{1}{\chi(\xi)^2} = \frac{8\pi}{\gamma}\frac{A\Phi^2}{\chi^3}\left[1+\frac{8\pi}{\gamma}(\xi-\xi_0)^2\,\Phi\cdot\left(\frac{3}{2}\frac{A\Phi}{\chi}-1\right)\right], \tag{35}$$

and

$$\frac{1}{\chi(\xi)}\frac{\partial^2}{\partial\xi^2}\frac{1}{\chi(\xi)^2} = \frac{8\pi}{\gamma}\frac{A\Phi^2}{\chi^4}\left[1+\frac{8\pi}{\gamma}(\xi-\xi_0)^2\,\Phi\cdot\left(\frac{3}{2}\frac{A\Phi}{\chi}-1\right)\right] \tag{36}$$

have to be determined. Examples are shown in Fig. 2b. The dependence of these derivatives on the *line strength* A is $\propto A$ for faint lines ($A \ll 1$), whereas very strong lines ($A \gg 1$) exhibit a proportionality $\propto 1/A$ for (33), $\propto 1/A^2$ for (34), (35),

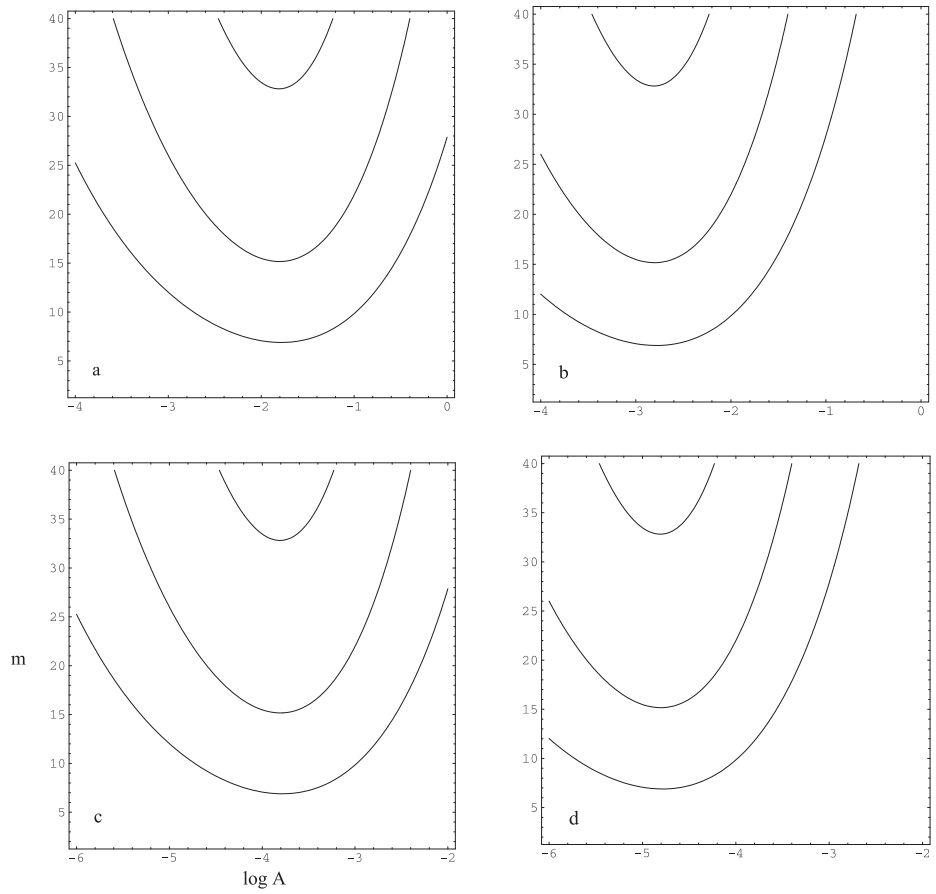

Fig. 3a–d. Relative accuracy $|\Upsilon_m - \Upsilon_\infty|/\Upsilon_\infty$ (cf. Eqs. (37), (43)) as a function of the line strength A and the "integration range" m for **a** $\gamma = 0.01$, **b** $\gamma = 10^{-3}$, **c** $\gamma = 10^{-4}$, and **d** $\gamma = 10^{-5}$. The *lower* curves indicate an accuracy of 10%, the *central* ones of 1%, and the *upper* ones of 0.1%.

and $\propto 1/A^3$ for (36). As the same also holds – for any finite m – for the corresponding integrated contributions, this behavior indicates that the effect of lines of *moderate* strength will be most important one.

For the subsequent discussion of several examples it is convenient to introduce the abbreviation

$$\Upsilon(\xi_a, \xi_b) = \int_{\xi_a}^{\xi_b} \frac{1}{\chi(\xi)} \frac{\partial^2}{\partial \xi^2} \frac{1}{\chi(\xi)^2}\, d\xi \tag{37}$$

for the (second order) *contribution* to the flux integrated over the interval $[\xi_a, \xi_b]$. Note that – in contrast to the coefficient η_2 (Eq. (21)) – Υ does not contain the weighting function G.

The contribution of a single Lorentzian line (on a continuum) to the wavelength-integrated quantities is obtained by integrating the derivatives over the line, i.e. over ξ from $\xi_0 - m\gamma/2$ to $\xi_0 + m\gamma/2$ where on the one hand $m > 0$ has to be sufficiently large, and on the other hand the weighting function G should not vary significantly with ξ. For the evaluation we utilize that the Lorentz profile is symmetric around ξ_0, i.e. $\Phi(\xi_0 + m\gamma/2) = \Phi(\xi_0 - m\gamma/2) = \Phi_m$, and hence also $\chi(\xi_0 + m\gamma/2) = \chi(\xi_0 - m\gamma/2) = \chi_m$. Then for the integral in the first-order coefficient (20) for the *total flux* obviously

$$\int_{\xi_0 - m\gamma/2}^{\xi_0 + m\gamma/2} \frac{\partial}{\partial \xi} \frac{1}{\chi(\xi)^2} d\xi = 0\,, \tag{38}$$

and – by using *Mathematica* – we find for the second-order coefficient (21)

$$\begin{aligned}
\Upsilon_m &= \Upsilon(\xi_0 - m\gamma/2, \xi_0 + m\gamma/2) \\
&= \int_{\xi_0 - m\gamma/2}^{\xi_0 + m\gamma/2} \frac{1}{\chi(\xi)} \frac{\partial^2}{\partial \xi^2} \frac{1}{\chi(\xi)^2} d\xi \\
&= -\frac{2\pi A^2}{\chi_c^2}\, m \left[\left(1 - \frac{\omega}{\varpi} - 4\left(1 - \frac{\omega}{A}\right)^2 \right) \frac{A}{\omega^4} - \frac{Z}{6\,\omega^3 \varpi} \right. \\
&\quad \left. + \frac{Z}{24\,\omega^2 \varpi^2} + \frac{Z}{16\,\omega \varpi^3} + \frac{Z}{16\,\varpi^4} \frac{\arctan(Xm)}{Xm} \right]
\end{aligned} \tag{39}$$

with Υ being defined by (37),

$$\begin{aligned}
\omega &= \frac{\chi_m}{\Phi_m} = A + (1 + m^2)\pi\chi_c\gamma/2\,, \\
\varpi &= \frac{\chi_0}{\Phi_0} = A + \pi\chi_c\gamma/2\,,
\end{aligned} \tag{40}$$

$$Z = 3A + 4\pi\chi_c\gamma\,, \tag{41}$$

and

$$X = \sqrt{\frac{\chi_c}{\chi_0}} = \sqrt{\frac{\pi}{2}\frac{\gamma\chi_c}{\varpi}}\,. \tag{42}$$

Φ_0 and χ_0 refer to the line center ($m = 0$).

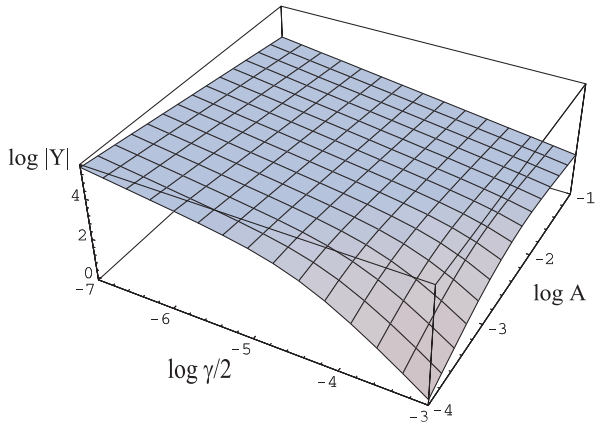

Fig. 4. Absolute value of the contribution $\Upsilon(-40\,\gamma, +40\,\gamma)$ for a single Lorentzian line on a continuum $\chi_c = 1$ as a function of A and γ. It is seen that $|\Upsilon|$ strongly increases with decreasing line width γ.

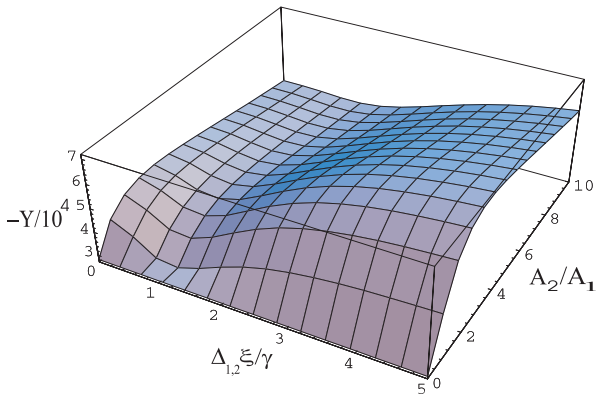

Fig. 5. Contribution $\Upsilon(-\infty, \infty)$ of two overlapping Lorentz lines to η_2 as a function of their relative strength A_2/A_1 and of their separation $\Delta_{12}\xi$ (in units of γ) for $\chi_c = 1$, $A_1 = 10^{-5}$, and – for both lines – $\gamma = 10^{-5}$.

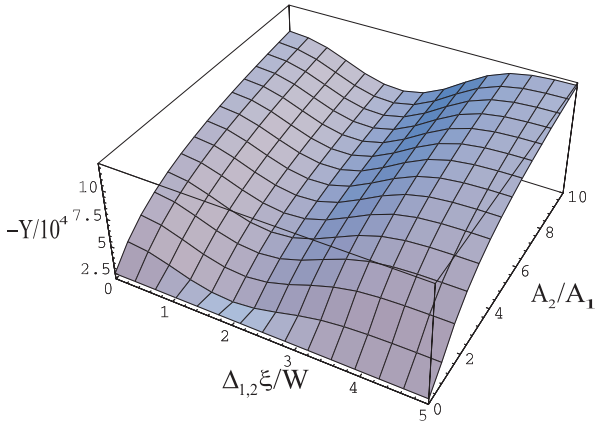

Fig. 6. Contribution $\Upsilon(-\infty, \infty)$ of two overlapping Gaussian lines (cf. Eq. (11)) to η_2 as a function of their relative strength A_2/A_1 and of ther separation $\Delta_{12}\xi$ (in units of W) for $\chi_c = 1$, $A_1 = 10^{-5}$, and – for both lines – a thermal width of $W = 10^{-5}$.

In the limit $m \to \infty$ we get for a fixed finite value of the line strength A

$$\Upsilon_\infty = \lim_{m\to\infty} \Upsilon_m = -\frac{\pi^{3/2}}{8\sqrt{2}} \frac{A^2 Z}{\sqrt{\gamma}\,\chi_c^{5/2}\varpi^{7/2}} < 0\,. \tag{43}$$

Note that in detail the dependence of X on A and m is rather involved. Its evaluation yields the following limiting cases

	$A \ll 1$	$A \gg 1$
m finite	$\propto A$	$\propto 1/A^3$
m infinite	$\propto A^2$	$\propto 1/\sqrt{A}$.

In Fig. 3 we show the dependence of $|\Upsilon_m - \Upsilon_\infty|/\Upsilon_\infty$ on A and m for four values of the damping constant γ in order to give a guideline to which distance from the line center, i.e. to which m, the integration over the line has to be carried out so that a sufficient accuracy of the second-order coefficient of the flux is achieved. It is seen that in every case one has to integrate far into the lines wings, i.e. to ξ values where the line contribution to the extinction coefficient has decreased to less than 1%. A *minimal* value of m can be used for lines with $A \approx \gamma$, for stronger and for weaker lines the relative contribution of the wings becomes more and more important and the integrations have to be extended further out.

The integrals contributing to the coefficients of the *total radiative acceleration* (23, 24) are

$$\int_{\xi_0-m\gamma/2}^{\xi_0+m\gamma/2} \frac{\partial}{\partial\xi}\frac{1}{\chi(\xi)}d\xi = 0\,, \tag{44}$$

$$\int_{\xi_0-m\gamma/2}^{\xi_0+m\gamma/2} \frac{\partial^2}{\partial\xi^2}\frac{1}{\chi(\xi)^2}d\xi = 8\pi\,\frac{A\Phi_m}{\chi_m^3}\cdot m > 0\,, \tag{45}$$

and furthermore

$$\lim_{m\to\infty}\int_{\xi_0-m\gamma/2}^{\xi_0+m\gamma/2} \frac{\partial^2}{\partial\xi^2}\frac{1}{\chi(\xi)^2}d\xi = 0 \tag{46}$$

since $\chi_m \to \chi_c$, and Φ_m decreases $\propto 1/m^2$ for $m \to \infty$.

The results derived in this subsection show that spectral lines – as long as they are isolated and have a symmetric shape – *only* contribute to the total *flux* in *second order* and not at all to the total acceleration (the latter being in strong contrast to the situation in optically thin or moderately thick situations). This implies that the differential motion in an optically very thick medium *reduces* $\mathcal{F}_{\rm tot}(s_0; w)$ via the effect of the (isolated, symmetric) lines or, equivalently, *in*creases the effective opacity $\bar{\chi}_\beta(s_0; w)$. This effect is *independent of the direction* of the flow (cf. Eq. (18)). Although effective only in second order, the influence of the lines on the flux may still be quite strong since usually there are very many lines. Note also that narrow lines of medium strength should be the most influential and that the importance decreases with increasing continuum opacity.

4.2.4. Many spectral lines

We first consider the case that the spectrum is dominated by *isolated* symmetric lines on a wavelength-independent continuum, i.e. that the line spacing is sufficiently large so that the lines do

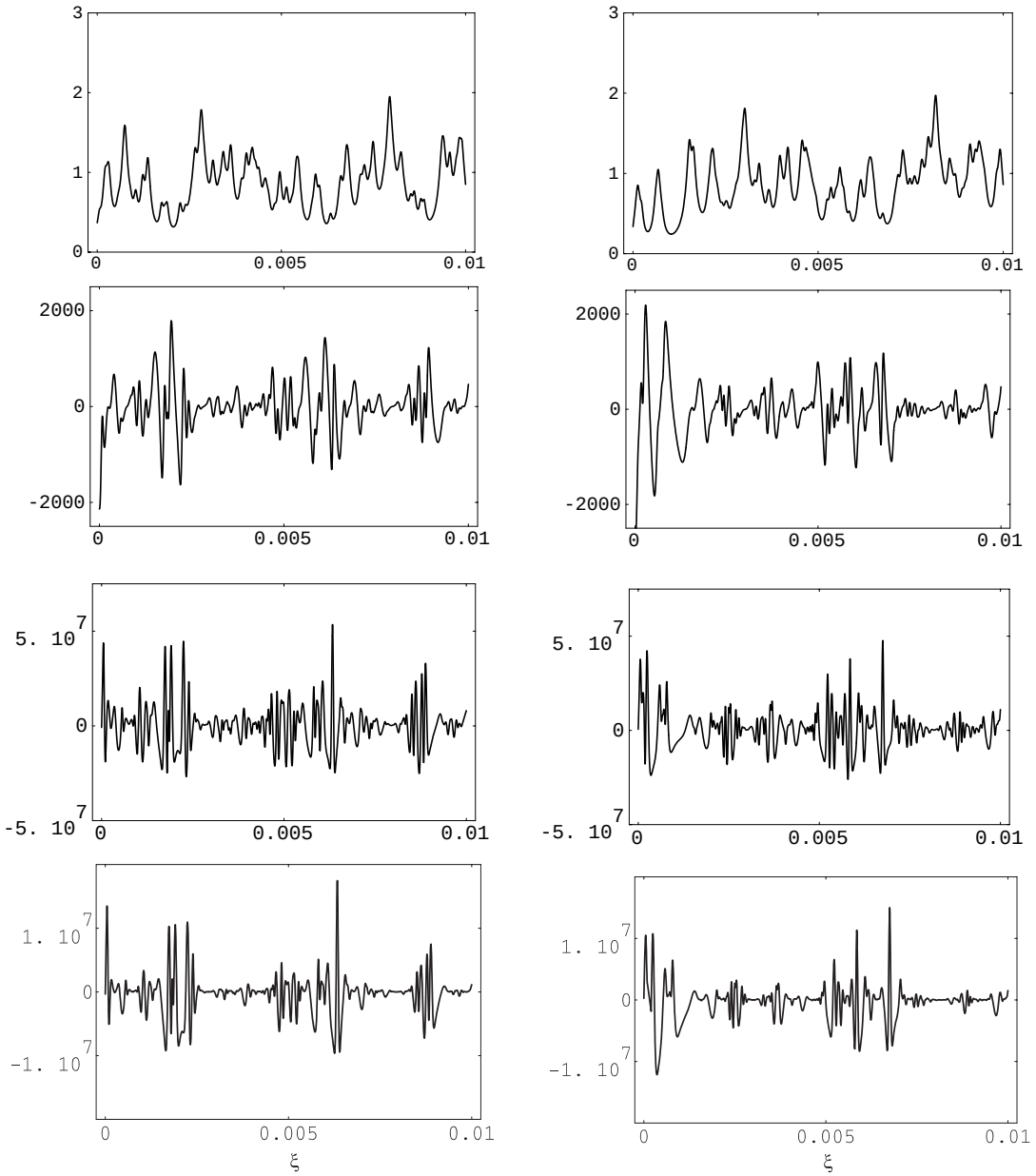

Fig. 7. Same as Fig. 2 but for two ensembles of 100 lines whose line centers are randomly distributed in the interval $0 \leq \xi \leq 0.01$ and whose strengths follow a logarithmic series distribution which is very similar to a power law with index $-3/2$. All lines have the same damping width $\gamma = 5 \cdot 10^{-5}$.

not essentially overlap and that the integration over each line in the limit $m \to \infty$, as described in Sect. 4.2.3, can effectively be carried out without interference with the neighboring lines. We furthermore assume that the weighting function G does not vary significantly over the integration range for each line. In this case the result of Sect. 4.2.3 holds that the only effect in a moving medium is to decrease the total flux in second order of w.

If on a flat continuum χ_c there are L (Lorentzian) lines, denoted by the index l, of strength A_l and width γ_l at the position ξ_l, only those spectral regions that are influenced by the lines contribute to the relevant integral in the coefficient $\eta_2(s_0)$ (Eq. (21)). Furthermore, for isolated lines the line-dominated portion of the spectrum is negligible compared to the line spacings so that the static Rosseland mean χ_R can be replaced by χ_c and hence approximately

$$\eta_2(s_0) \approx \frac{1}{2}\chi_c \sum_{l=1}^{L} G(s_0, \xi_l)\Upsilon_{\infty,l} \tag{47}$$

with the abbreviation

$$\Upsilon_{\infty,l} = -\frac{\pi^{3/2}}{8\sqrt{2}} \frac{A_l^2 Z_l}{\sqrt{\gamma_l}\,\chi_c^{5/2}\varpi_l^{7/2}} \tag{48}$$

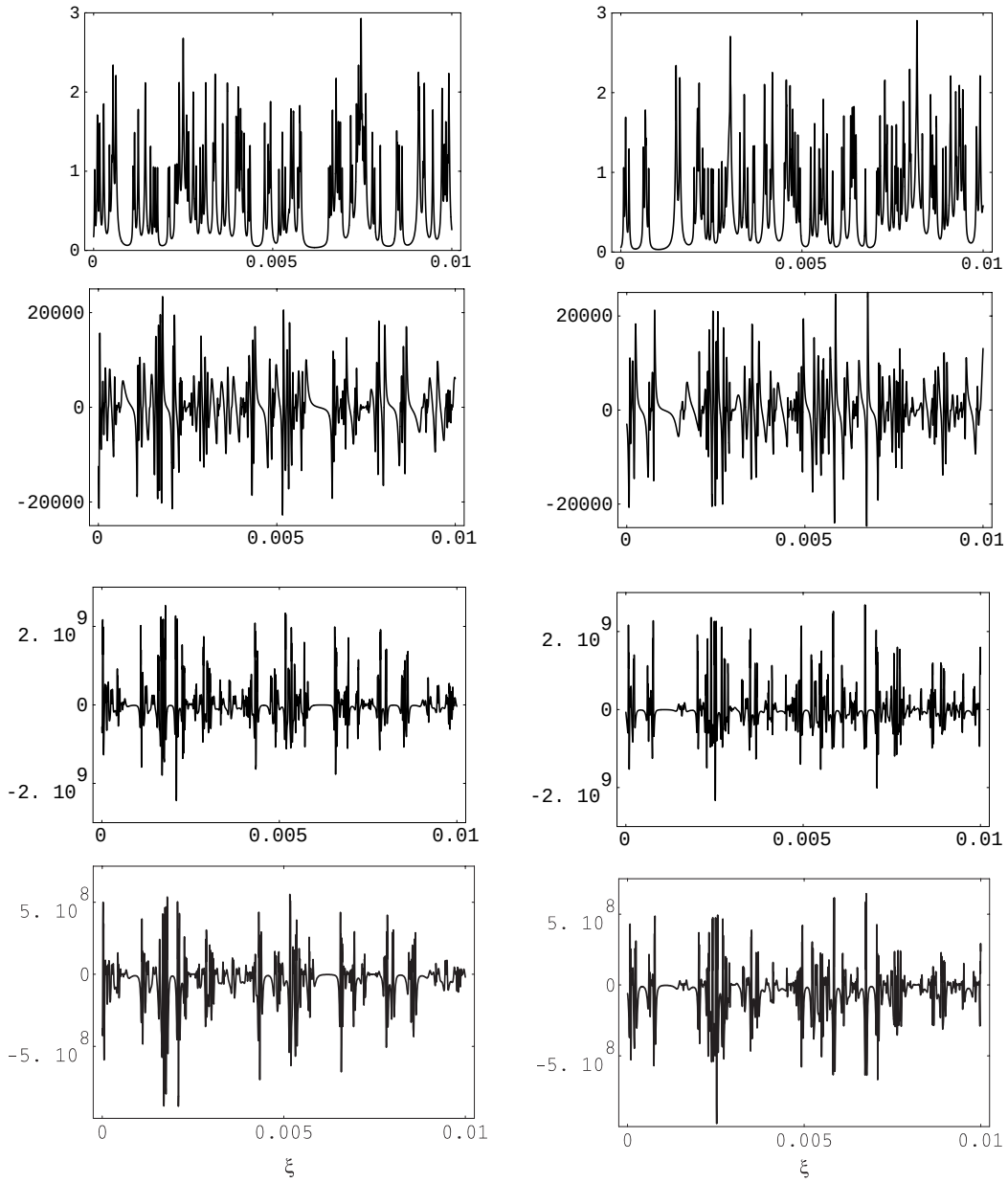

Fig. 8. Same as Fig. 7 but for $\gamma = 5 \cdot 10^{-6}$. Note the strongly changed vertical scales.

as given by Eq. (43), and Z_l and ϖ_l defined by (41) and (40), respectively.

In the special case of L spectral lines with *identical* A_l and γ_l (and hence Z_l, ϖ_l, and $\Upsilon_{\infty,l}$) Eq. (47) reads

$$\eta_2(s_0) \approx \frac{1}{2}\chi_c \sum_{l=1}^{L} G(s_0, \xi_l) \cdot \Upsilon_\infty \,. \tag{49}$$

This expression is valid for any number L of lines as long as they do not overlap. If, however, in addition we assume that there are many lines, i.e. $L \gg 1$, distributed over the spectrum in such a way that the trapezoidal integration rule gives a sufficiently accurate result for the integral $\int G d\xi$, we can further evaluate the sum. For this it is required that the *line density* ϱ, i.e. the number of lines per unit ξ-interval, or, equivalently, the line separation $\Delta\xi \approx 1/\varrho$ is roughly constant over the relevant part of the spectrum. Then

$$\int_{-\infty}^{\infty} G(s_0,\xi) d\xi \approx \sum_{l=1}^{L} G(s_0,\xi_l) \cdot \Delta\xi \approx \frac{1}{\varrho} \sum_{l=1}^{L} G(s_0,\xi_l) \,, \tag{50}$$

and hence

$$\eta_2(s_0) \approx \frac{1}{2}\, \chi_c\, \varrho\, \Upsilon_\infty \tag{51}$$

since the weighting function is normalized according to $\int_{-\infty}^{\infty} G(s_0,\xi) d\xi = 1$.

An extinction coefficient which is more realistic than that for isolated lines comprises *overlapping* spectral lines and hence *asymmetric* features. The complexity of the effects already

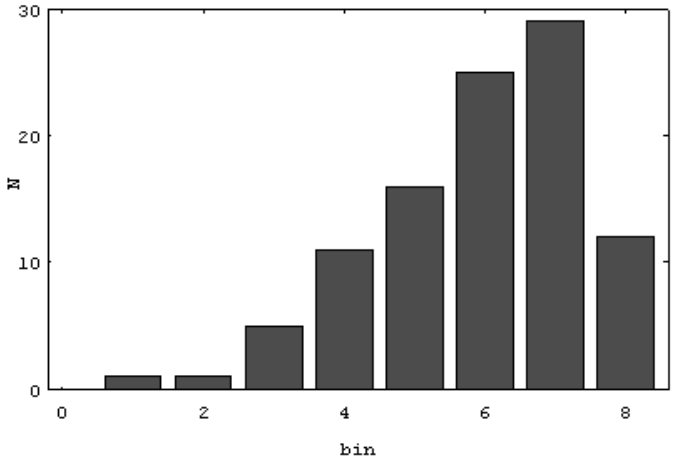

Fig. 9. Distribution of $\Upsilon(0, 0.01)$ for 100 Lorentzian lines on a continuum $\chi_c = 1$ with randomly chosen central wavelengths (100 realisations) and a logarithmic series distribution of strengths. The bins of which each has a width of $\Delta\Upsilon = 500$ cover the range $-6500 \le \Upsilon \le -2500$. The mean value is $\langle\Upsilon\rangle = -3804$ with a standard deviation of 748.

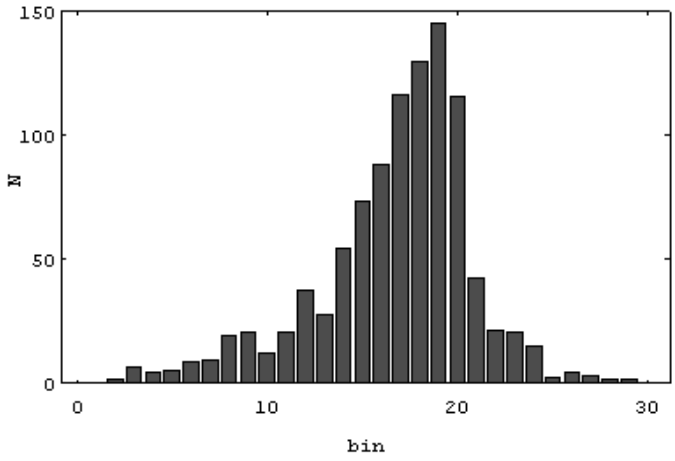

Fig. 10. Distribution of $\Upsilon\Big(0.001\,i, 0.001\,(i{+}1)\Big)$ with $i = 0 \ldots 9$ for the lines described in Fig. 9, but with the integrations extended over *subintervals* of $\delta\xi = 0.001$. The bins with a width $\Delta\Upsilon = 100$ cover the range $-2000 \le \Upsilon \le +1000$. The mean value is $\langle\Upsilon\rangle = -380$ with a standard deviation of 416.

shows up already in the very simple case of *two* overlapping lines if their relative strength and separation are varied (cf. Figs. 5, 6).

As can be seen from from Figs. 7 and 8, the situation gets even more intricate whenever several lines overlap. However, it is obvious that the strong dependence on the damping – seen already for a single line – is maintained and that the contribution to the ξ-integrals are largest from regions of weak absorption with large gradients.

In order to get some impression of the variations of Υ resulting from line shifts we generated 100 random realisations of central wavelengths for 100 lines in the interval $0 \le \xi \le 0.01$ and determined $\Upsilon(0, 0.01)$ numerically. As is seen from Fig. 9 the resulting values of $\Upsilon(0, 0.01)$ may vary strongly with an asymmetric distribution. However, all values stay negative as is expected from the discussion of single lines. This need not be correct if the integration is restricted to smaller spectral regions (cf. Fig. 10) covering a smaller number of lines (on the average 10 in our case): then the fluctuations are much larger and even positive values of η_2 may occur (though with low probability).

5. The flux vector in moving 3D media

It is obvious from Eqs. (4) and (5) that the direction dependence of w induces a complicated dependence of the flux vector $\mathbf{F}_{\rm tot}$ (I:11) on the directions of the velocity vector and of the temperature gradient. In particular, it appears possible that in case these directions do not coincide there is a flux component perpendicular to the temperature gradient.

While it seems impossible to derive an explicit expression for the flux vector analytically in the general case, this could be done in the limit of small $|w|$. However, even in this case the general expressions are quite lengthy and very difficult to interpret.

In order to discuss the essential effects we therefore consider here as example a *plane-parallel* medium with a temperature gradient in the normal direction (taken to be the z-direction) and with a velocity field ($\beta \ll 1$) which is assumed to vary only with the z coordinate in the neighborhood of the point s_0 of interest, i.e. in cartesian coordinates

$$\nabla T = \begin{pmatrix} 0 \\ 0 \\ dT/dz \end{pmatrix}, \qquad \boldsymbol{\beta} = \begin{pmatrix} 0 & 0 & b_x \\ 0 & 0 & b_y \\ 0 & 0 & b_z \end{pmatrix} \begin{pmatrix} x \\ y \\ z \end{pmatrix}. \quad (52)$$

For the direction $\mathbf{n} = (n_x, n_y, n_z)$ one now obtains from Eq. (2)

$$w = n_z\,(n_x b_x + n_y b_y + n_z b_z)\,, \quad (53)$$

and the integration over all directions (see Eq. I:12) of Eq. (18) yields

$$\mathbf{F}_{\rm tot} = \frac{4\pi}{3}\,\frac{1}{\bar{\chi}_{\rm R}}\,\frac{\partial B}{\partial T}\,\frac{dT}{dz} \quad (54)$$
$$\times \left\{ \begin{pmatrix} 0 \\ 0 \\ 1 \end{pmatrix} + \frac{1}{5}\,\eta_1 \begin{pmatrix} b_x \\ b_y \\ 3\,b_z \end{pmatrix} + \frac{3}{35}\,\eta_2 \begin{pmatrix} 2\,b_x b_z \\ 2\,b_y b_z \\ b_x^2 + b_y^2 + 5\,b_z^2 \end{pmatrix} \right\}$$

where all coefficients are to be taken at s_0.

It is seen that the classical result for static media is fully regained for $b_x = b_y = b_z = 0$. If the velocity vector is in the z direction ($b_x = b_y = 0$), i.e. if it is parallel to the temperature gradient, the x and y components of the flux vector are still zero, but the z component is modified by the velocities as has been discussed in Sect. 4.1:

$$\mathbf{F}_{\rm tot} = \frac{4\pi}{3}\,\frac{1}{\bar{\chi}_{\rm R}}\,\frac{\partial B}{\partial T}\,\frac{dT}{dz}\,\left(0,\ 0,\ 1 + \frac{3}{5}\,\eta_1\,b_z + \frac{3}{7}\,\eta_2\,b_z^2\right). \quad (55)$$

The coefficients of the η terms are just given by the two angle averages $\langle\cos^4\vartheta\rangle\,/\,\langle\cos^3\vartheta\rangle = 3/5$ and $\langle\cos^6\vartheta\rangle\,/\,\langle\cos^3\vartheta\rangle = 3/7$, respectively.

If the flow direction and the temperature gradient are *not* parallel ($b_x,\ b_y \neq 0$), the comparison of Eq. (55) with (54) shows

that the flux component in z direction is not changed in first order but it is increased in second order. More significantly, however, we find also non-zero flux components in the x and y directions, i.e. there is now a radiative flux perpendicular to the temperature gradient.

6. Conclusions and outlook

The expressions derived in this paper show that inside of an optically very thick, differentially moving medium the total flux and the total radiative acceleration in the limits of large and small velocity gradients w are given on the one hand by simple functions of w and on the other by expressions that depend on the plasma properties only and that therefore can be precalculated without any knowledge of the velocity field. For large w, essentially, a wavelength average of the extinction coefficient enters. For the more important case of small w, the free mean path is of primary importance as in the static case, i.e. regions of low opacity contribute most. This is in contrast to optically thin or partially thick configurations such as e.g. stellar winds. The Doppler shifts lead to ξ derivatives, and since these enter the flux and radiative acceleration in a highly non-linear way, predictions even of the signs of the effects (as e.g. the change of the flux with velocity) are uncertain without the knowledge of specific details. We have therefore concentrated the analysis in this paper on very simple spectral features and investigated a few more complicated systems only numerically.

An alternative to this approach – which in addition provides a way for *understanding* systems comprising many spectral lines – is to represent the line positions, strengths, and shapes by a *statistical* model and then solve the corresponding stochastic equations. This will be done for a Poisson point process in a subsequent paper.

Acknowledgements. We are indebted to G.V. Efimov, Ph. Rosenau, G. Kanschat and G. Shaviv for many helpful discussions. This work has been supported in part by the DFG (Sonderforschungsbereich 359/C2).

References

Baschek B., Grüber C., von Waldenfels W., Wehrse R., 1997, A&A 320, 920
Wehrse R., Baschek B., 1999, Physics Reports 311, 187
Wehrse R., Baschek B., von Waldenfels W., 2000, A&A (Paper I).
Wehrse R., von Waldenfels W., Baschek B., 1998, JQSRT 60, 963